Bull. Chem. Soc. Jpn. Vol. 81, No. 4, 521–524 (2008)

High-Trivalent Rare Earth Ion Conduction in Solids Based on NASICON-Type Phosphate

Yasunori Hasegawa,[1] Shinji Tamura,[2] Mineo Sato,[1] and Nobuhito Imanaka*[2]

[1]Department of Chemistry and Chemical Engineering, Faculty of Engineering, Niigata University,
8050 Ikarashi 2 no-cho, Niigata 950-2181

[2]Department of Applied Chemistry, Faculty of Engineering, Osaka University, 2-1 Yamadaoka, Suita, Osaka 565-0871

Received September 18, 2007; E-mail: imanaka@chem.eng.osaka-u.ac.jp

Trivalent rare earth ion conductors of the $(R_{0.05}Zr_{0.95})_{80/79}Nb(PO_4)_3$ (R: rare earths) series with NASICON-type structures were successfully prepared and the optimum size of ion-conducting pathways for rare earth ions in $(R_{0.05}Zr_{0.95})_{80/79}Nb(PO_4)_3$ solids was investigated. The most suitable ion-conducting pathway for rare earth ion conduction in this series was realized for R = Dy and the highest conductivity of $3.2 \times 10^{-4}\,S\,cm^{-1}$ at 600 °C was obtained for $(Dy_{0.05}Zr_{0.95})_{80/79}Nb(PO_4)_3$ solids. Since R^{3+} ion conduction was strongly dependent on the ratio of conducting R^{3+} ion size to crystal lattice size ($V_{R^{3+}}/V_{lattice}$; we denote this ratio as *A* ratio in this article), it was clear that the *A* ratio is a key factor to optimize R^{3+} ion conduction in NASICON-type structures.

Solid electrolyte is a functional material in which only single ion species conduct in solids accompanying electric charge. This is different from electronic conducting solids such as metals and semiconductors whose charge carrier is electrons or holes. Because of this outstanding characteristic, solid electrolytes are greatly expected to be applied to various kinds of electrochemical devices such as chemical sensors and all solid-state-type rechargeable batteries.[1,2] Up to now, many kinds of mono- and divalent ion conducting solids have been developed, and among them, Na^+ ion conducting β-alumina and O^{2-} ion conducting yttria-stabilized zirconia have been already commercialized as key components of Na/S batteries (sodium/sulfur batteries, which consist of sodium at the negative electrode and sulfur at the positive electrode separated by a β-alumina solid electrolyte) for electric power storage and oxygen sensors for vehicle emission control, respectively. In contrast, trivalent ions have been regarded as poor migrant species in solids because of the strong electrostatic interaction between the trivalent ion and the lattice forming anions surrounding the trivalent ion.

In order to realize trivalent ion conduction in solids, the framework of the solid electrolyte should possess a large conducting pathway enough for migration of the relatively bulky trivalent ion. In addition, it is also necessary to reduce the above-mentioned strong electrostatic interaction by introducing higher valence cations than the trivalent state into the structure. Furthermore, contamination by cations lower than trivalent should be avoided because mono- or divalent cations can easily migrate in solids compared with the target trivalent cations.

Since 1999, pure trivalent cation conducting $R_{1/3}Zr_2(PO_4)_3$ (R = Sc, Y, and Eu–Lu)[3–7] solid electrolytes with a NASICON[8] ($\underline{Na}^+$ super ionic conductor, which is a tailored solid electrolyte and has a three-dimensional network structure where PO_4 tetrahedra and ZrO_6 octahedra are linked by sharing corner oxygens) structure have been successfully developed by the above-described concepts. Although the $R_{1/3}Zr_2(PO_4)_3$ solids contain high-valence cations of Zr^{4+} and P^{5+} and have NASICON-type structures,[9] their trivalent ion conductivities in $R_{1/3}Zr_2(PO_4)_3$ solids are considerably lower than those of commercially available divalent oxide anion conductors such as yttria-stabilized zirconia (YSZ)[10] and calcia-stabilized zirconia (CSZ)[10] due to low crystallinity which results from low thermal stability (the decomposition temperature of the $R_{1/3}Zr_2(PO_4)_3$ solids: ca. 950 °C), indicating that they are not satisfactory for practical application. Moreover, the single phase of the NASICON-type $R_{1/3}Zr_2(PO_4)_3$ solids were obtained for only some rare earth ions with small ionic radius (0.0885–0.1087 nm).

Recently, we have successfully improved trivalent rare earth R^{3+} ion conduction in NASICON-type solids for $(R_xZr_{1-x})_{4/(4-x)}Nb(PO_4)_3$ (R = La–Nd and Gd; $x = 0.1$) solids,[11–13] whose electrostatic interaction between the conducting trivalent R^{3+} ion and the surrounding oxide anions was intentionally reduced by additionally introducing a pentavalent Nb^{5+} cation into the $R_{1/3}Zr_2(PO_4)_3$ framework as the constituent high-valent cation. These solids exhibited considerably high-trivalent R^{3+} ion conductivity, which was comparable to those of the representative divalent oxide anion conductors of YSZ and CSZ. However, while a few light rare earth ion species have been demonstrated to migrate in $(R_{0.1}Zr_{0.9})_{40/39}Nb(PO_4)_3$ solids, heavy rare earth ion conducting solid electrolytes have not been obtained for this composition ($x = 0.1$ in $(R_xZr_{1-x})_{4/(4-x)}Nb(PO_4)_3$) because the ionic size of heavy rare earths are too small to hold the single phase of the NASICON structure in this composition and the resulting materials were usually a multi-phase mixture of NASICON-type solids, $NbPO_5$, and RPO_4.

In this study, for the purpose of systematically investigating the trivalent ion conducting characteristics in NASICON-type solids, we have synthesized a single phase of NASICON-type

Published on the web April 10, 2008; doi:10.1246/bcsj.81.521

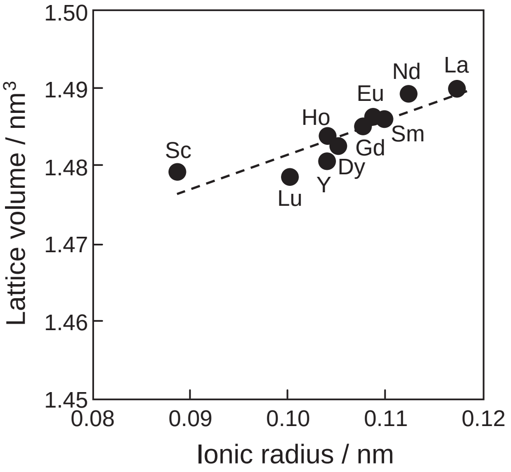

Figure 1. The trivalent R^{3+} ionic radius dependence of the lattice volume for the $(R_{0.05}Zr_{0.95})_{80/79}Nb(PO_4)_3$ solids.

$(R_{0.05}Zr_{0.95})_{80/79}Nb(PO_4)_3$ (R = rare earths: Sc, Y, La, Nd, Sm, Eu, Gd, Dy, Ho, and Lu) solids, whose conducting trivalent cation species were from the smallest Sc^{3+} to the largest La^{3+}, by reducing the rare earth ion concentration (x) from 0.1 to 0.05 in $(R_xZr_{1-x})_{4/(4-x)}Nb(PO_4)_3$, and ion conducting properties in the $(R_{0.05}Zr_{0.95})_{80/79}Nb(PO_4)_3$ series were studied.

Experimental

$(R_{0.05}Zr_{0.95})_{80/79}Nb(PO_4)_3$ (R = Sc, Y, La, Nd, Sm, Eu, Gd, Dy, Ho, and Lu) solids were prepared from R_2O_3 (R = Sc, Y, Nd, Sm, Eu, Gd, Ho, and Lu) (99.9%), $R_2(SO_4)_3\cdot 8H_2O$ (R = Dy) (99.99%) or $R(NO_3)_3\cdot 6H_2O$ (R = La) (99.99%), ZrO_2 (99.99%), Nb_2O_5 (99.99%), and $(NH_4)_2HPO_4$ (99.99%). Starting materials were mixed in an agate pot at a rotation speed of 300 rpm for 6 h by ball milling (Pulverisette 7, FRITSCH GmbH). The mixed powder was pelletized and heated at 600 °C for 12 h, and then 1300 °C for 12 h in air. The resulting powder was made into pellets and sintered on an alumina plate at 1300 °C for 12 h in air. The samples obtained were identified by X-ray powder diffraction (XRD) using Cu Kα radiation (MultiFlex, Rigaku). The lattice parameters were calculated by refining the XRD patterns using α-Al_2O_3 standard powder. Thermogravimetric and differential thermal analysis measurements (TG-DTA, DTG-50H, Shimadzu) were performed with a heating rate of 3 °C min^{-1}. Electrical conductivity of the samples was measured by an ac method, using the sintered sample pellet with two Pt electrodes. The ac conductivity measurement was performed by a complex impedance method using a Precision LCR meter (4192A, Hewlett Packard) in a frequency range between 5 Hz and 13 MHz at temperatures from 600 to 300 °C in air.

Results and Discussion

All $(R_{0.05}Zr_{0.95})_{80/79}Nb(PO_4)_3$ (R = Sc, Y, La, Nd, Sm, Eu, Gd, Dy, Ho, and Lu) solids prepared were confirmed to possess the same single-phase rhombohedral ($R\bar{3}c$) NASICON-type structure as $NaZr_2(PO_4)_3$ (typical NASICON-type Na^+ ion conductor) from XRD analysis. The lattice volumes of all samples are depicted in Figure 1 as a function of trivalent ionic radius. The lattice volume monotonically expands with increasing R^{3+} ionic radius, indicating formation of a solid solution.

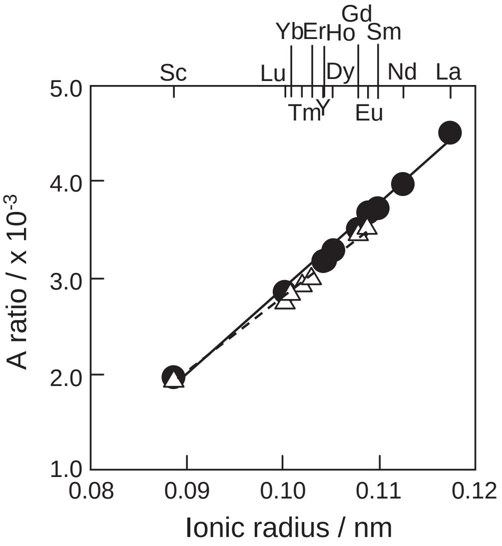

Figure 2. The R^{3+} ionic radius dependencies of the A ratio for the $(R_{0.05}Zr_{0.95})_{80/79}Nb(PO_4)_3$ solids (●) and the $R_{1/3}Zr_2(PO_4)_3$ solids (△). The A ratio shows the ratio of the trivalent R^{3+} ionic size to the lattice volume ($V_{R^{3+}}/V_{\mathrm{lattice}}$).

These results show that NASICON-type $(R_{0.05}Zr_{0.95})_{80/79}Nb(PO_4)_3$ solids were successfully obtained for a series of rare earth ions from the smallest Sc^{3+} to the largest La^{3+} while the conducting ion species in the conventional trivalent ion conductors $R_{1/3}Zr_2(PO_4)_3$ and $(R_{0.1}Zr_{0.9})_{40/39}Nb(PO_4)_3$ were limited to heavy or light rare earth ions, respectively.

From the thermogravimetric analyses for the $(R_{0.05}Zr_{0.95})_{80/79}Nb(PO_4)_3$ series, all the $(R_{0.05}Zr_{0.95})_{80/79}Nb(PO_4)_3$ solids were found to be stable up to 1300 °C, the same as the previously reported $(R_{0.1}Zr_{0.9})_{40/39}Nb(PO_4)_3$ series.[13] Since the $R_{1/3}Zr_2(PO_4)_3$ solids decomposed at ca. 950 °C, it was clear that the thermal stability of the NASICON-type trivalent rare earth cation conductors was greatly improved by introducing the pentavalent Nb^{5+} cation into the lattice, which caused the formation of strong bonds between Nb^{5+} cation and the lattice forming O^{2-} anions.

Figure 2 shows the trivalent ionic radius dependence of the A ratio ($V_{R^{3+}}/V_{\mathrm{lattice}}$)[14] for the $(R_{0.05}Zr_{0.95})_{80/79}Nb(PO_4)_3$ solids, which is defined as the ratio of the migrating trivalent cation volume ($V_{R^{3+}}$) to the crystal lattice volume (V_{lattice}). The corresponding data of conventional NASICON-type $R_{1/3}Zr_2(PO_4)_3$ solids are also depicted in the same figure. The A ratios monotonically decrease with reducing trivalent ionic radius for both series, and the values are almost the same for each trivalent R^{3+} ion species. Furthermore, change in A ratio slope for both series is also the same, which indicates that similar lattice volume change occurs for both series by changing R^{3+} ionic size. These phenomena appear by the countervailing effect of lattice shrinkage by substituting the Zr^{4+} (0.086 nm; 6-coordinate)[15] site with smaller Nb^{5+} (0.078 nm; 6-coordinate)[15] in the solid and lattice expansion due to the decrease of R–O bonding that is caused by the reduction of R^{3+} cation concentration.

The A ratio dependencies of the conductivity at 600 °C for $(R_{0.05}Zr_{0.95})_{80/79}Nb(PO_4)_3$ solids and $R_{1/3}Zr_2(PO_4)_3$ series are depicted in Figure 3a. The conductivity of the

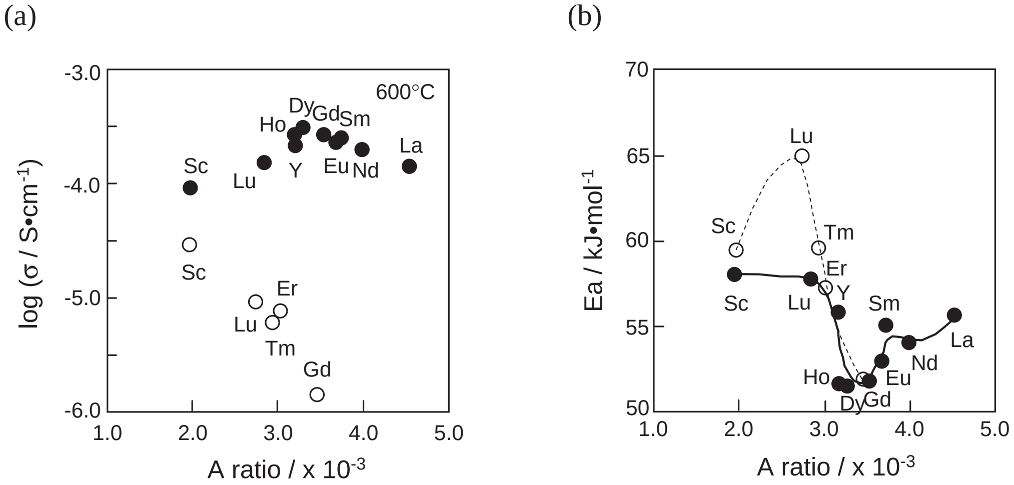

Figure 3. (a) The *A* ratio dependence of the conductivity at 600 °C for the $(R_{0.05}Zr_{0.95})_{80/79}Nb(PO_4)_3$ solids (●) with the corresponding data of the $R_{1/3}Zr_2(PO_4)_3$ solids (○). (b) The *A* ratio dependence of the activation energies for $(R_{0.05}Zr_{0.95})_{80/79}Nb(PO_4)_3$ solids (●) with the corresponding data of the $R_{1/3}Zr_2(PO_4)_3$ solids[7] (○).

$(R_{0.05}Zr_{0.95})_{80/79}Nb(PO_4)_3$ solids depends on the *A* ratio ($V_{R^{3+}}/V_{\mathrm{lattice}}$) and $(Dy_{0.05}Zr_{0.95})_{80/79}Nb(PO_4)_3$ (A ratio $= 3.29 \times 10^{-3}$) shows the highest conductivity of 3.2×10^{-4} $\mathrm{S\,cm^{-1}}$ among the samples prepared. For *A* ratio regions smaller than that of R = Dy, the trivalent R^{3+} ion conducting pathway, which is strongly related to lattice volume, becomes larger with decreasing *A* ratio. In such a large conducting pathway, the R^{3+} ion cannot be located at the center of the ion pathway by the strong electrostatic interaction with the nearest lattice-forming oxide anions, resulting in the decrease of ion conduction. On the other hand, with increasing the *A* ratio from Dy^{3+} to La^{3+}, the conductivity decreased due to contraction of the trivalent ion conducting pathway. From this result, it becomes clear that the most suitable *A* ratio for trivalent R^{3+} ion conduction in the $(R_{0.05}Zr_{0.95})_{80/79}Nb(PO_4)_3$ series is obtained for R = Dy. In contrast, the optimum *A* ratio for trivalent R^{3+} ion conduction is realized for R = Sc in the $R_{1/3}Zr_2(PO_4)_3$ series, which has a smaller ionic radius than Dy^{3+}. In the case of the $R_{1/3}Zr_2(PO_4)_3$ series, the highest ion conductivity was obtained for the smallest Sc^{3+} due to the small bottleneck which is caused by the strong R–O bonds in the NASICON-type framework. On the other hand, for the $(R_{0.05}Zr_{0.95})_{80/79}Nb(PO_4)_3$ series, the R–O bonds were weakened by the high-valent Nb^{5+} cation in the $R_{1/3}Zr_2(PO_4)_3$ lattice, resulting in enlargement of the bottleneck. Furthermore, as we described before, lowering the R^{3+} concentration also help to enlarge the bottleneck, and the most suitable interaction between R^{3+} and O^{2-} was obtained for the larger ion species of Dy^{3+} compared to Sc^{3+}. As a result, the trivalent Dy^{3+} ion can be located at the center of the ion pathway, achieving the most suitable ion conducting circumstance for R = Dy in the $(R_{0.05}Zr_{0.95})_{80/79}Nb(PO_4)_3$ series.

Figure 3b presents the *A* ratio dependencies of the activation energies (E_a) for ion conduction for the $(R_{0.05}Zr_{0.95})_{80/79}Nb(PO_4)_3$ and $R_{1/3}Zr_2(PO_4)_3$ series, which are calculated from the $\log(\sigma T)$–$1/T$ relationship. Since the $(Dy_{0.05}Zr_{0.95})_{80/79}Nb(PO_4)_3$ solid possesses the lowest activation energy in addition to the highest ion conductivity in the NASICON-type $(R_{0.05}Zr_{0.95})_{80/79}Nb(PO_4)_3$ series, the Dy^{3+} ion is in such a circumstance to conduct most smoothly in solids. This result clearly supports the idea that the optimum ion conducting pathway in the $(R_{0.05}Zr_{0.95})_{80/79}Nb(PO_4)_3$ series was obtained for R = Dy. Furthermore, although the R^{3+} ion concentration in $(R_{0.05}Zr_{0.95})_{80/79}Nb(PO_4)_3$ series is lower than that in $R_{1/3}Zr_2(PO_4)_3$, the $(R_{0.05}Zr_{0.95})_{80/79}Nb(PO_4)_3$ series shows both higher conductivity and lower E_a. These results indicate that the R^{3+} ion conduction in the $(R_{0.05}Zr_{0.95})_{80/79}Nb(PO_4)_3$ solids becomes easier by introducing the high-valent Nb^{5+} ion in the crystal lattice, which can reduce the electrostatic interaction between R^{3+} and O^{2-} ions.

Conclusion

Trivalent rare earth ion conducting NASICON-type $(R_{0.05}Zr_{0.95})_{80/79}Nb(PO_4)_3$ (R: rare earths) solid electrolytes were successfully developed for a variety of rare earth ions from the smallest Sc^{3+} to the largest La^{3+}. Among the NASICON-type $(R_{0.05}Zr_{0.95})_{80/79}Nb(PO_4)_3$ solids, the most suitable trivalent rare earth ion conducting pathway was found to be obtained for R = Dy from the relationship between the *A* ratio ($V_{R^{3+}}/V_{\mathrm{lattice}}$) and the trivalent R^{3+} ion conductivity. Since the R^{3+} ion conductivity depends on the *A* ratio, the *A* ratio is one of the key factors to optimize the individual ion conduction in the NASICON-type phosphate series.

This work was supported by the "Research Fellowships of the Japan Society for the Promotion of Science for Young Scientists." This work was also partially supported by the Industrial Technology Research Grant Program in '05 (Project ID: 05A18011d) from the New Energy and Industrial Technology Development Organization (NEDO) of Japan, and by the Hyogo Science and Technology Association and the Yazaki Memorial Foundation for Science & Technology.

Supporting Information

Brief identification methods of the trivalent R^{3+} ion conduction in the $(R_{0.05}Zr_{0.95})_{80/79}Nb(PO_4)_3$ (R: rare earths) solids. This material is available free of charge on the web at http://www.csj.jp/journals/bcsj/.

References

1 T. Kudo, K. Fueki, *Solid State Ionics*, Kodansha, Tokyo, **1990**.

2 P. G. Bruce, *Solid State Electrochemistry*, Cambridge University Press, Cambridge, **1995**.

3 S. Tamura, N. Imanaka, G. Adachi, *Adv. Mater.* **1999**, *11*, 1521.

4 S. Tamura, N. Imanaka, G. Adachi, *Solid State Ionics* **2000**, *136–137*, 423.

5 S. Tamura, N. Imanaka, G. Adachi, *J. Alloys Compd.* **2001**, *323–324*, 540.

6 S. Tamura, N. Imanaka, G. Adachi, *Chem. Lett.* **2001**, 672.

7 S. Tamura, N. Imanaka, G. Adachi, *J. Mater. Sci. Lett.* **2001**, *20*, 2123.

8 J. B. Goodenough, H. Y.-P. Hong, J. Kafaras, *Mater. Res. Bull.* **1976**, *11*, 203.

9 M. A. Talbi, R. Brochu, C. Parent, L. Rabardel, G. Le Flem, *J. Solid State Chem.* **1994**, *110*, 350.

10 D. W. Strickler, W. G. Carlson, *J. Am. Ceram. Soc.* **1964**, *47*, 122.

11 Y. Hasegawa, N. Imanaka, G. Adachi, *J. Solid State Chem.* **2003**, *171*, 387.

12 Y. Hasegawa, S. Tamura, N. Imanaka, G. Adachi, Y. Takano, T. Tsubaki, K. Sekizawa, *J. Alloys Compd.* **2004**, *375*, 212.

13 Y. Hasegawa, N. Imanaka, *J. Alloys Compd.* **2006**, *408–412*, 661.

14 H. Aono, N. Imanaka, G. Adachi, *Acc. Chem. Res.* **1994**, *27*, 265.

15 R. D. Shannon, *Acta Crystallogr., Sect. A* **1976**, *32*, 751.